

1 **Electro-oxidative depolymerisation of technical lignin in water using**  
2 **platinum, nickel oxide hydroxide and graphite electrodes**

3

4 **Nicola Di Fidio**<sup>a</sup>, **Johan W. Timmermans**<sup>b</sup>, **Claudia Antonetti**<sup>a</sup>, **Anna Maria**  
5 **Raspolli Galletti**<sup>a</sup>, **Richard J. A. Gosselink**<sup>b</sup>, **Roel J. M. Bisselink**<sup>b\*</sup>, **Ted M.**  
6 **Slaghek**<sup>b\*</sup>.

7 <sup>a</sup> *Department of Chemistry and Industrial Chemistry, University of Pisa, Via G. Moruzzi*  
8 *13, 56124 Pisa, Italy.*

9 <sup>b</sup> *Wageningen Food and Biobased Research, Wageningen University & Research,*  
10 *Bornse Weilanden 9, 6708 WG Wageningen, Netherlands*

11

12 \*Corresponding author: Roel J. M. Bisselink

13 E-mail address: roel.bisselink@wur.nl

14 Telephone: +31 317483871

15

16 \*Co-corresponding author: Ted M. Slaghek

17 E-mail address: ted.slaghek@wur.nl

18 Telephone: + 31 317481977

19

20 **ABSTRACT**

21 In order to improve the lignin exploitation to added-value bioproducts, a mild chemical  
22 conversion route based on electrochemistry was **investigated**. For the first time, soda  
23 lignin Protobind™ 1000 (technical lignin from the pulp & paper industry) was studied  
24 by cyclic voltammetry to **preliminarily** investigate the effect of the main reaction

25 parameters, such as the type of electrode material (platinum, nickel oxide hydroxide,  
26 graphite), the pH (12, 13, 14), the scan rate (10, 50, 100, 250 mV/s), the substrate  
27 concentration (2, 20 g/L) and the oxidation/reduction potential (from -0.8 to +0.8 V).  
28 Under the optimal reaction conditions **among those tested** (NiOOH electrode, pH 14,  
29 lignin 20 g/L, 0.4 V), the electro-oxidative depolymerisation of lignin by electrolysis  
30 was performed in a divided cell. The reaction products were identified and quantified by  
31 ultra-pressure liquid chromatography coupled with mass spectrometry. The main  
32 products were sinapic acid, vanillin, vanillic acid, and acetovanillone. The obtained  
33 **preliminary** results demonstrated the potential feasibility of this innovative  
34 electrochemical route for lignin valorisation for the production of bio-aromatic  
35 chemicals.

36  
37 **Keywords:** Soda lignin Protobind™ 1000, Electrochemical oxidation, NiOOH  
38 electrode, Bio-aromatics, Vanillin.

## 40 **1. Introduction**

41 Among renewable resources, low-cost and abundantly available lignocellulosic  
42 biomass plays a fundamental role in the bio-based and circular economy.  
43 Lignocellulosic biomass is mainly composed of three biopolymers: cellulose,  
44 hemicellulose and lignin. Cellulose is the most abundant biopolymer in the world. The  
45 second one is lignin which represents a promising and renewable source of aromatic  
46 compounds.<sup>1</sup> In order to promote the economic sustainability and profitability of  
47 biorefinery models, the full exploitation of the starting feedstock should be pursued by  
48 the conversion of all its components into added-value molecules and/or materials.<sup>2</sup>

49 In this perspective, the valorisation of technical lignins, which represent one side-  
50 stream of the existing industrial-scale biorefineries and paper industry, is a strategic  
51 approach to enhance the biorefinery and paper industry sustainability.<sup>3</sup> Side-streams of  
52 pulp & paper industry are rich in technical lignin, due to the almost complete  
53 valorisation of hemicellulose and cellulose components. In the present preliminary  
54 investigation, the soda technical lignin Protobind™ 1000 (P1000) was adopted as  
55 starting material. P1000 lignin is produced on an industrial scale by the company  
56 GreenValue, starting from a mix of wheat straw and Sarkanda grass. It is obtained by  
57 alkaline extraction from biomass with sodium hydroxide.<sup>4</sup> In the literature, numerous  
58 studies propose several interesting approaches for lignin upgrading, such as pyrolysis,  
59 enzymatic or chemical depolymerisation and surface functionalisation.<sup>5-9</sup> However,  
60 most of them require harsh reaction conditions, such as high temperature, high pressure,  
61 expensive and hazardous catalysts which make the process not economically viable on a  
62 larger scale.<sup>10</sup> The electrochemical depolymerisation of lignin, especially if powered by  
63 renewable electricity, is a promising technology compared to conventional chemical  
64 oxidation because it can operate under mild, safe and eco-friendly reaction conditions,  
65 such as room temperature and atmospheric pressure.<sup>11</sup> Among electrochemical  
66 approaches, the electro-oxidation of lignin at the anode is the most common one  
67 studied.<sup>12</sup> Even if electrocatalytic approaches similar to that adopted in the present study  
68 were reported in the literature for other combinations of lignins and working  
69 electrodes,<sup>13-15</sup> investigations regarding the electrochemical conversion of P1000 lignin,  
70 up to now, are absent. Only a few studies are available concerning its chemical  
71 valorisation through inorganic catalysts, such as CuMgAlO<sub>x</sub> or NiMo sulphide, in  
72 organic solvents under harsh reaction conditions.<sup>16-18</sup>

73 During the electrochemical oxidation of lignin, the surface functionalisation ( $\alpha$ -  
74 carbonylation) and the cleavage of C-C/C-O bonds are the two main competing  
75 reactions.<sup>19</sup> In particular, the cleavage of  $\beta$ -O-4 linkages is considered the rate-  
76 determining step in lignin depolymerization.<sup>20, 21</sup> Mechanistic studies demonstrated that  
77 the C-O bond of the  $\beta$ -O-4 aryl ether linkage and C $\alpha$ -C $\beta$  bonds could be cleaved by  
78 electrocatalysts.<sup>21, 22</sup>

79 In the literature, the direct electro-oxidation of technical lignins was performed using  
80 Ni, Pb/PbO<sub>2</sub>, Ti/SnO<sub>2</sub>, Sb<sub>2</sub>O<sub>3</sub>, RuO<sub>2</sub>-IrO<sub>2</sub>/Ti electrodes as catalysts, namely as working  
81 electrode (anode) or as an immobilised coating on the surface of the electrode.<sup>23-26</sup> The  
82 present **preliminary** investigation, for the first time, is aimed to assess the performances  
83 of Pt, Ni/NiOOH and graphite as electrode materials for the P1000 lignin electro-  
84 oxidative depolymerisation. One of the main limitations in the scaling-up of  
85 electrochemical approaches could be the high cost of metal electrodes or electrode  
86 coatings, if for example Pt-based electrodes are involved.<sup>27</sup> Thus, a challenging effort is  
87 represented by the development of electrochemical processes based on low-cost  
88 electrocatalysts,<sup>12</sup> justifying the choice of graphite and nickel in the present work. In  
89 detail, a preliminary investigation of the performances of three different electrode  
90 materials (Pt, Ni/NiOOH and graphite) for the P1000 lignin electro-oxidative  
91 depolymerisation was performed by cyclic voltammetry adopting different reactions  
92 conditions, such as pH 12, 13 and 14, lignin concentration 2 and 20 g/L, scan rates 10,  
93 50, 100 and 250 mV/s. Moreover, in order to validate the catalytic performances of the  
94 selected electrodes, the cyclic voltammetry study was also performed on guaiacol,  
95 considered as a model compound of a prominent lignin structural unit. Finally, the most

96 efficient electrode and the optimal reaction conditions **among those tested** were then  
97 adopted in the electrolysis of soda P1000 lignin into added-value aromatic compounds.

98

## 99 **2. Materials and methods**

### 100 **2.1 Chemicals and materials**

101 The commercially available soda lignin Protobind™ 1000 (P1000) was provided by  
102 GreenValue S.A. (Switzerland). It has been obtained from a mixture of wheat straw and  
103 Sarkanda grass. A detailed characterisation of P1000 lignin is described in previous  
104 work,<sup>4</sup> which has the chemical composition of (wt% on dry matter): glucan  $0.5 \pm 0.2$ ,  
105 xylan  $1.5 \pm 0.1$ , galactan  $0.2 \pm 0.0$ , arabinan  $0.2 \pm 0.2$ , mannan  $< 0.1$ , rhamnan  $< 0.1$ ,  
106 acid-insoluble lignin  $85.1 \pm 0.7$ , acid-soluble lignin  $5.4 \pm 0.0$ , ash  $2.5 \pm 0.0$ , other  
107 compounds  $4.6 \pm 1.2$ .

108 HPLC-grade water and acetonitrile were products of Brunschwig Chemie  
109 (Amsterdam, The Netherlands). Formic acid (98-100%) was purchased from Riedel-de  
110 Haën (Seelze, Germany). The phenolics were obtained from Sigma-Aldrich (St. Louis,  
111 MO, USA). Milli-Q water was used throughout for preparation of all eluents and  
112 standard solutions. All other reagents and compounds were of the available highest  
113 purity.

114 Three working electrode materials were tested in the present investigation: Pt wire  
115 (geometric area =  $1.0 \text{ cm}^2$ , Metrohm), Ni/NiOOH wire (geometric area =  $0.37 \text{ cm}^2$ ,  
116 Sigma Aldrich), graphite rod (geometric area =  $1.0 \text{ cm}^2$ , Alfa Aesar).

117

### 118 **2.2 NiOOH electrode preparation**

119 A layer of NiOOH was formed on a nickel substrate in an electrochemical cell  
120 having a three-electrode configuration. The working electrode was a Ni wire ( $l = 1.15$   
121  $\text{cm}$ ,  $d = 0.1 \text{ cm}$ , geometric area =  $0.37 \text{ cm}^2$ ), which was washed with ethanol, acetone  
122 and demi-water prior to the electrochemical treatment. As counter electrode a platinum  
123 wire ( $l = 20 \text{ cm}$ ,  $d = 0.025 \text{ cm}$ , geometric area =  $1.57 \text{ cm}^2$ ) was used. An Ag/AgCl  
124 electrode (Radiometer Analytical REF201) was used as a reference electrode.

125 The electrolyte solution was composed of  $0.05 \text{ M NiSO}_4$ ,  $0.1 \text{ M CH}_3\text{COONa}$  and  
126  $0.005 \text{ M NaOH}$  at room temperature. The thickness of the deposited oxides was  
127 controlled via applied current. Thus, to get a layer of around  $0.4 \cdot 10^{-6} \text{ g}$ , six consecutive  
128 potentiometric cycles or 12 steps ( $0.5 \text{ mA cm}^{-2}$ ,  $60 \text{ s}$ ) were applied.<sup>28</sup> After the  
129 preparation, the Ni electrode was rinsed with ethanol and demi-water.

130

### 131 **2.3 Cyclic voltammetry**

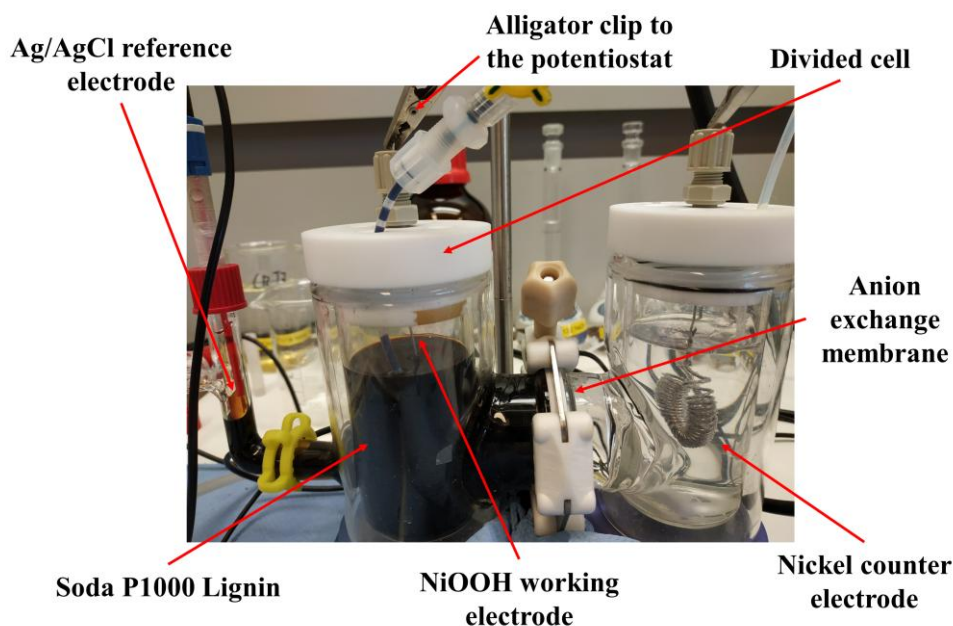
132 Cyclic voltammetry (CV) was used in order to examine electrocatalytic properties of  
133 various electrode materials for the electro-oxidative depolymerisation of P1000 lignin.  
134 The experimental setup consisted of an undivided electrochemical cell linked to a  
135 potentiostat (Ivium Technologies, the Netherlands), Pt wire as a counter electrode and  
136 Ag/AgCl electrode (Radiometer Analytical REF201) as a reference electrode. The  
137 following materials were tested as working electrode: Pt wire, Ni/NiOOH wire and  
138 graphite rod. All electrodes were used as purchased, except Ni/NiOOH, which was  
139 pretreated to deposit NiOOH layer on the electrode (see Sect. 2.2). Investigated  
140 electrolyte solutions were composed of  $0.01 \text{ M NaOH} + 0.99 \text{ M NaClO}_4$  (pH 12),  $0.10$   
141  $\text{M NaOH} + 0.90 \text{ M NaClO}_4$  (pH 13),  $1.0 \text{ M NaOH}$  (pH 14). The electrochemical cell  
142 contained  $50 \text{ mL}$  of solution. Argon gas was purged in the electrolyte solution before

143 the measurements in order to remove oxygen. The CV measurements were performed at  
144 room temperature (20 °C). All the currents reported in this work were normalised with  
145 respect to the geometric area of the electrodes. Different scan rates (10, 50, 100, 250  
146 mV/s) were investigated modulating the potentiostat. Eight full cycles were performed  
147 for the scan rate of 10 mV/s, fifteen full cycles were performed for the scan rate of 50  
148 and 100 mV/s, while twenty-five full cycles were performed for the scan rate of 250  
149 mV/s. In order to investigate the effect of the substrate concentration on the  
150 electrocatalytic properties, two values of lignin concentration, 2 and 20 g/L, were tested.

151

## 152 **2.4 Electro-oxidative depolymerisation**

153 Electrolysis of P1000 lignin was performed in a custom-made double-walled divided  
154 electrochemical glass cell in a three-electrode configuration under galvanostatic  
155 conditions (6.4 mA/cm<sup>2</sup>) using a potentiostat (Fig. 1). The current was measured  
156 through the potentiostat obtaining the value of 150 mA. Then it was correlated to the  
157 geometric area of the NiOOH working electrode (23.55 cm<sup>2</sup>) used in the electrolysis.  
158 Based on this calculation, the current density was 6.4 mA/cm<sup>2</sup>.



159

160 **Fig. 1** Picture of the custom-made double-walled divided electrochemical glass cell in a  
 161 three-electrode configuration used for the electrolysis of soda P1000 lignin under the  
 162 optimal reaction conditions.

163

164 The electrochemical cell contained 150 mL catholyte (1.0 M NaOH, pH 14), 150 mL  
 165 anolyte (1.0 M NaOH, pH 14, 20 g/L P1000 lignin). It was divided by an anion  
 166 exchange membrane, with a dry thickness of 130  $\mu\text{m}$  (Fumasep<sup>®</sup> FAA-3-PK-130,  
 167 Fumatech). Prior to use, the membrane was immersed in an aqueous solution of 1 M  
 168 NaOH for 24 h at room temperature, in order to exchange the bromide ( $\text{Br}^-$ ) counter ions  
 169 into hydroxyl ( $\text{OH}^-$ ). The presence of an anion exchange membrane ensured the  
 170 diffusion of  $\text{OH}^-$  ions from the catholyte solution to the anolyte one, which made  
 171 negligible the variation of pH in presence of a low concentration of phenolic products.  
 172 Argon gas was purged in anolyte and catholyte solutions prior to and during the reaction  
 173 in order to completely remove oxygen in the electrochemical cell thus avoiding the



174 involvement of the atmospheric oxygen in the investigated reaction. Both compartments  
175 were stirred and electrolysis was performed at room temperature. The three-electrode  
176 configuration consisted of the Ni counter electrode ( $l = 75$  cm,  $d = 0.1$  cm, geometric  
177 area =  $23.55$  cm<sup>2</sup>), the Ag/AgCl reference electrode (Radiometer Analytical REF201)  
178 via a Luggin capillary and the Ni/NiOOH working electrode ( $l = 75$  cm,  $d = 0.1$  cm,  
179 geometric area =  $23.55$  cm<sup>2</sup>). Counter and working electrodes were spirally wound to fit  
180 into the electrochemical cell. Around 4 mL of the catholyte was used to fill the Luggin  
181 capillary and reservoir into which the Ag/AgCl reference electrode was placed.  
182 Electrolysis was carried out at 0.4 V vs. Ag/AgCl for 4 h. The anolyte and catholyte  
183 solutions were separately collected after electrolysis. The lignin-containing solution was  
184 then analysed by UPLC/MS analysis.

185 The theoretical electrochemical conversion (%) was calculated as the ratio between  
186 the consumed moles of electrons during electrolysis and the theoretical amount of moles  
187 of electrons required for the complete electrolysis of the starting lignin (3 g). For the  
188 calculation of this last factor, the monomer average molecular weight of 195.2 g/mol  
189 and 4 electrons consumed per mole were considered according to the literature.<sup>29</sup>

190

## 191 **2.5 UPLC/MS analysis**

192 Samples from the electrochemical divided cell were neutralised with formic acid and  
193 centrifuged in order to separate the unreacted lignin and the insoluble high molecular  
194 weight oligomers. Then, the liquid fraction was recovered by microfiltration (0.22  $\mu$ m  
195 filter). The UPLC/MS analysis was performed by a Dionex RSLC system with an  
196 UltiMate 3000 Rapid Separation pump and auto-sampler. The detector was a Dionex  
197 Ultimate 3000 RS Diode Array Detector (280 nm) in combination with a Thermo

198 Scientific<sup>TM</sup> LCQ Fleet Ion Trap Mass spectrometer. The separating column was a  
199 Waters Acquity UPLC BEH C18 reversed-phase column (1.7  $\mu$ m particle size, 2.1  $\times$   
200 150 mm) with a sample loop of 100  $\mu$ L. The guard column was a Waters VanGuard  
201 Acquity UPLC BEH C18 guard column (1.7  $\mu$ m particle size, 2.1  $\times$  5 mm).

202 The column temperature was maintained at 40 °C. Eluent A consisted of Biosolve  
203 ULC/MS grade water with 1 mL/L formic acid (MS for positive and negative modus).  
204 Eluent B consisted of Biosolve ULC/MS grade acetonitrile. Elution was performed at a  
205 flow rate of 0.35 mL/min, using the following gradient (expressed as solvent B, while  
206 solvent A is the complementary part): initial composition 4.0% B; 0.0-1.0 min 4.0% B;  
207 1.0-17.0 min 56.0% B; 17.0-20.0 min 70.0% B; 20.0-24.0 min 100% B; 24.0-30.0 min  
208 4.0% B. Heated electrospray ionization (HESI) mass spectrometry was performed in  
209 both positive and negative modes. The LCQ mass spectrometer was operated with the  
210 HESI set on 150 °C and the capillary temperature at 235 °C, sheath gas at 20 arbitrary  
211 units, the auxiliary gas at 5 arbitrary units and the sweep gas at 4 arbitrary units. The  
212 electrospray voltage was set to 5.0 kV. In the positive modus, the capillary voltage was  
213 set at 11.0 V and the tube lens offset at 45.0 V. In the negative modus the capillary  
214 voltage was set at -1.0 V and the tube lens offset at -44.9 V. The injection time was 100  
215 ms. Mass spectra were recorded from m/z 70-500 at a unit mass resolution without in-  
216 source fragmentation. For sequential MS/MS experiments the normalised collision  
217 energy was 35%, with wideband activation turned off.

218 Standard (stock) solutions were obtained by weighing the phenolics of interest (with  
219 analytical precision, on an analytical balance) in a volumetric flask (50 or 100 mL) and  
220 subsequently adding/dissolving the phenolics in a mixture of methanol and Milli-Q-  
221 water (50:50 v/v). Trans-Cinnamic acid (for phenolic acids) and 1-Methyl-naphthalin (for

222 phenolics) were used as internal standards (I.S.). For sample preparation, 500  $\mu\text{L}$   
223 sample (or standard solution) was mixed with 500  $\mu\text{L}$  I.S., mixed and transferred into a  
224 1.0 mL Dionex vial, to be ready for analysis. All the structural identifications were  
225 confirmed by using authentic aromatic standards. Retention times, UV-vis spectra, and  
226 MS/MS spectra of the compounds were matched with those of the corresponding  
227 commercial standards

228

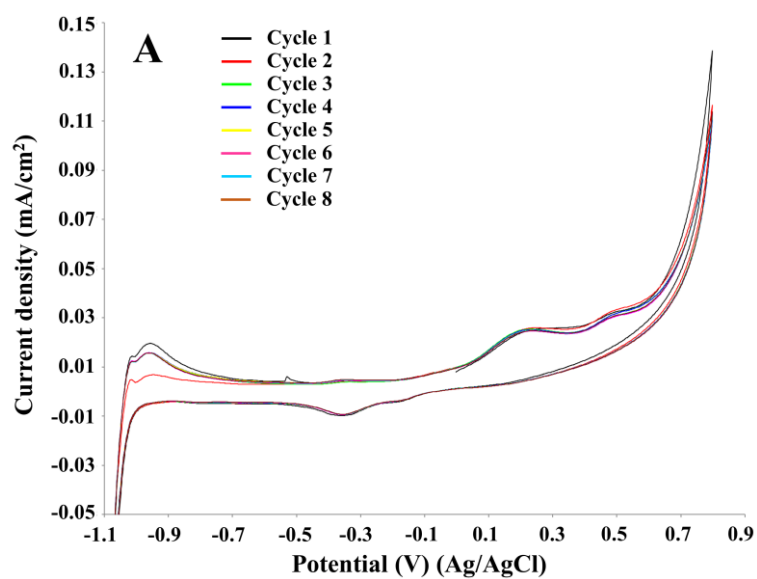
### 229 **3. Results and discussion**

#### 230 **3.1 Cyclic voltammetry study - effect of the electrocatalyst**

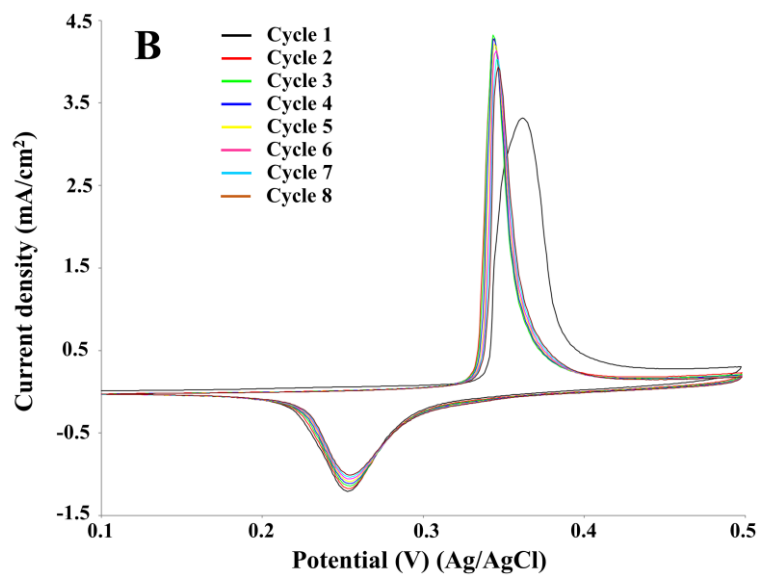
231 In electrochemical reactions based on direct electro-oxidation of lignin, the anode  
232 material and structure, especially in terms of surface features, plays a crucial role in the  
233 process performance.<sup>30</sup> The electrocatalyst should be both stable towards anodic  
234 corrosion and passivation, and catalytically effective for lignin depolymerisation. A  
235 preliminary investigation on the Pt, NiOOH and graphite electrodes was performed by  
236 cyclic voltammetry in order to identify the oxidation potential of P1000 lignin in the  
237 electrolyte as a function of pH and the kind of electrocatalyst and to evaluate the  
238 optimal reaction conditions in terms of the electrode, pH and lignin concentration.

239 Eight full cycles were performed with the scan rate of 10 mV/s for the three  
240 electrodes, as showed in Fig. 2. In all the cases the last and the second cycles were  
241 similar, thus confirming limited electrode passivation during the cyclic voltammetry  
242 experiments. The same behaviour of nickel and graphite electrodes in the cyclic  
243 voltammetry of Kraft lignin was observed by Di Marino et al.<sup>14</sup> In the first cycle on Pt  
244 and graphite electrodes two oxidation peaks were observed at ca. 0.2 and 0.5 V.

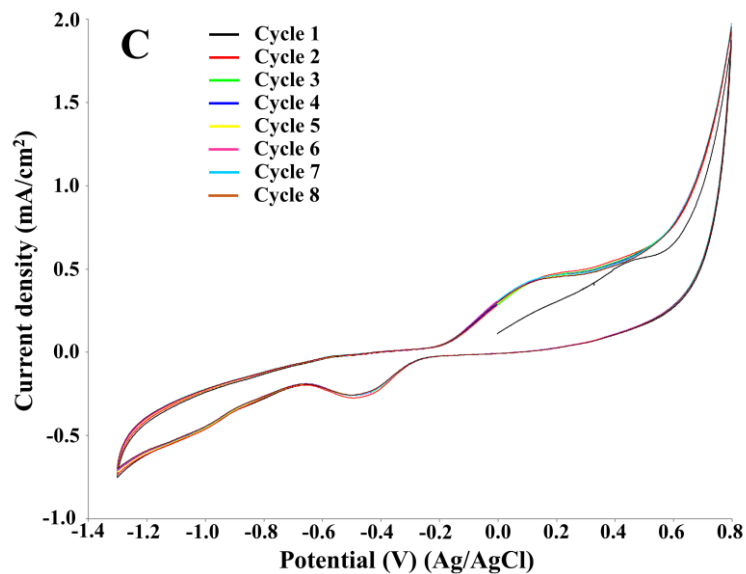
245 According to Milczarek,<sup>31</sup> in the first anodic scan the second oxidation peak at higher  
246 potential value is related to the irreversible oxidation.



247



248

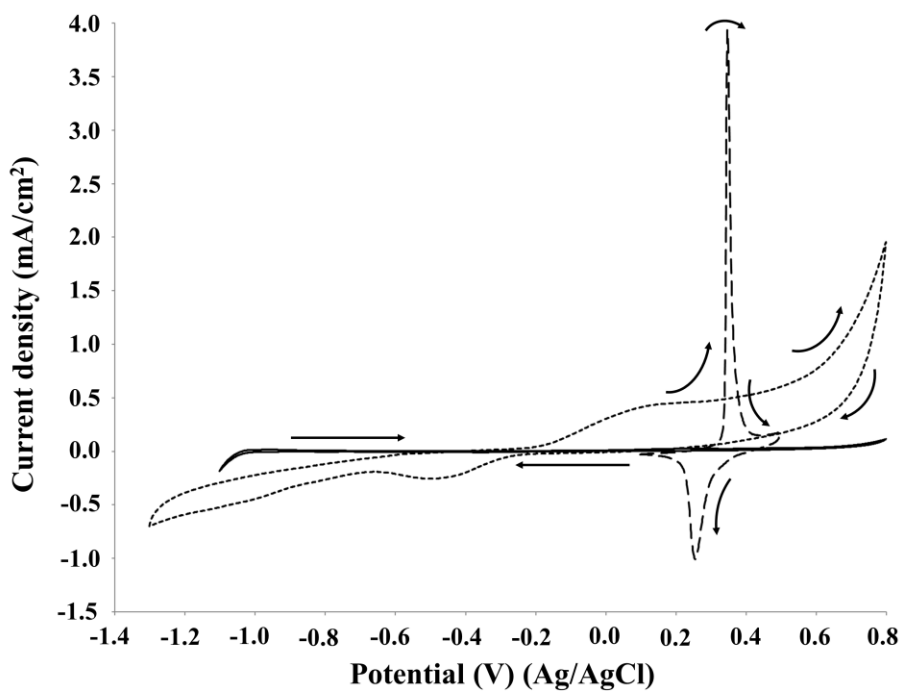


249

250 **Fig. 2** Cyclic voltammetry of 2 g/L P1000 lignin in 1 M NaOH (pH 14).  
 251 Voltammograms recorded at 10 mV/s on platinum (A), NiOOH (B), and graphite (C)  
 252 electrodes at room temperature.

253

254 Fig. 3 compares the results obtained by cyclic voltammetry of soda P1000 lignin (2  
 255 g/L) on Pt, NiOOH and graphite electrodes at pH 14.



256

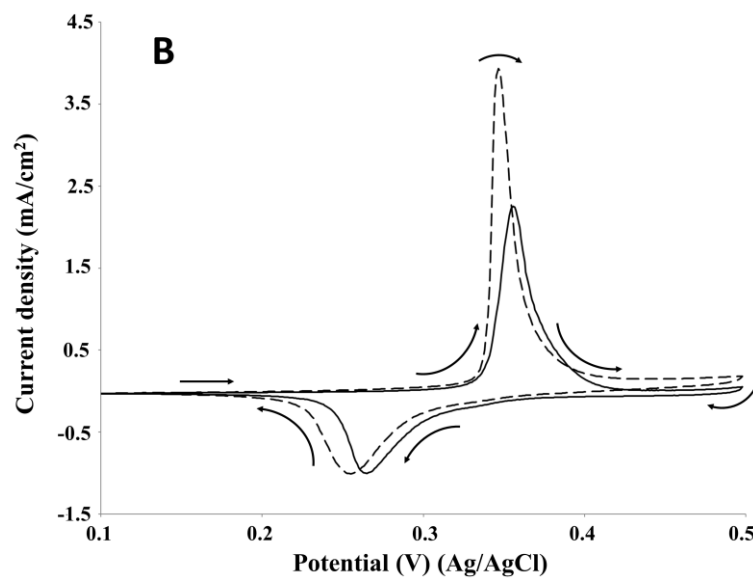
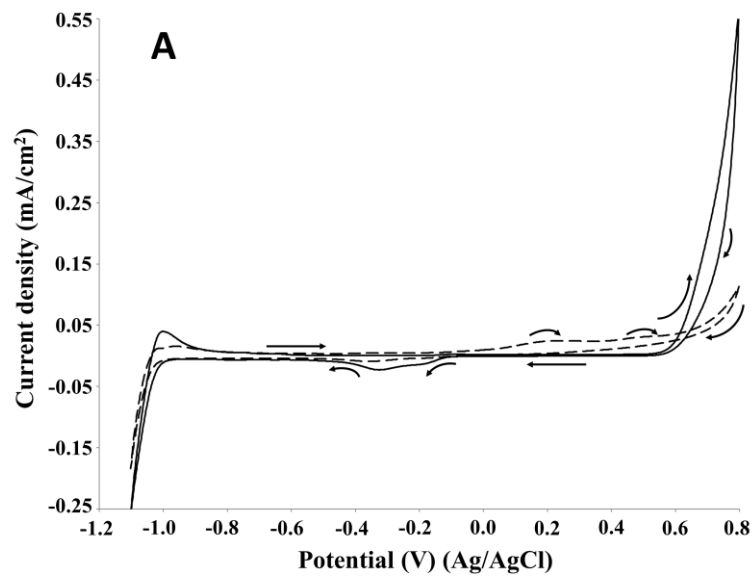
257 **Fig. 3** Cyclic voltammetry of 2 g/L P1000 lignin in 1 M NaOH (pH 14).  
258 Voltammograms recorded at 10 mV/s at room temperature. Solid line: on platinum  
259 electrode; dashed line: on NiOOH electrode; dotted line: on graphite electrode.

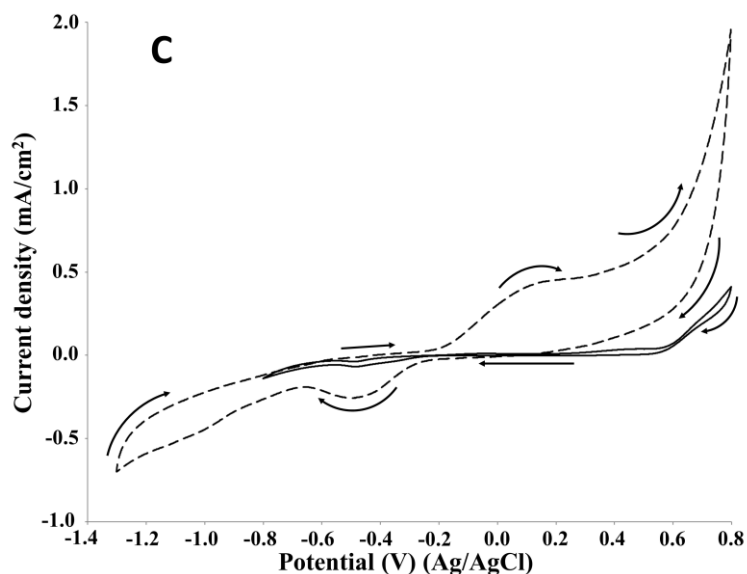
260

261 The profiles obtained on platinum, nickel oxide hydroxide and graphite electrodes differ  
262 considerably. In all the cases one or two oxidation peaks were observed between 0.2 and  
263 0.5 V. Similar results were obtained by Parpot et al.<sup>32</sup> for the electro-oxidation of Kraft  
264 lignin on Ni and Pt electrodes and by Movil-Cabrera et al.<sup>33</sup> on Co core/Pt partial shell  
265 nanoparticle alloy electrocatalyst. Moreover, the potential value of 0.45 V was obtained  
266 by Caravaca et al. for the electro-oxidation of Kraft lignin on bimetallic Pt-Ru anode.<sup>34</sup>

267 For each electrode material, the current density increased significantly compared to  
268 the control (no lignin) as can be seen in Fig. 4. In particular, on Pt electrode (Fig. 4A)  
269 two oxidation peaks were observed at 0.2 and 0.5 V. Differently, on NiOOH (Fig. 4B)  
270 and graphite (Fig. 4C) electrodes only one oxidation peak was ascertained: in the first  
271 case it was around 0.35 V, while in the second case it was around 0.2 V. Regarding the  
272 lignin reactivity, on Pt electrode the current density increased to around  $23 \mu\text{A}/\text{cm}^2$  at  
273 0.2 V and around  $28 \mu\text{A}/\text{cm}^2$  at 0.5 V with respect to the control test. On NiOOH  
274 electrode the current density increased to around  $2 \text{ mA}/\text{cm}^2$  at 0.35 V, while on graphite  
275 electrode it increased to around  $0.5 \text{ mA}/\text{cm}^2$  at 0.2 V. Moreover, in the presence of  
276 lignin, on NiOOH electrode the charge density, namely the supplied charge related to  
277 the electrode area, of the oxidation and reduction peaks were  $9.8$  and  $6.1 \text{ mC}/\text{cm}^2$ ,  
278 respectively. In the absence of lignin, namely in the control test, the charge density of  
279 the oxidation and reduction peaks were  $6.3$  and  $5.5 \text{ mC}/\text{cm}^2$ , respectively. Thus, the net  
280 charge density in the oxidation sweep was  $3.5 \text{ mC}/\text{cm}^2$ , corresponding to an increase of

281 about 56% respect to the control test. The net charge density in the reduction sweep was  
282 only  $0.6 \text{ mC/cm}^2$ , corresponding to an increase of about 10% respect to the control test.  
283 On this basis, the electrochemical oxidation of lignin in alkaline medium resulted an  
284 irreversible reaction.  
285 By comparing the results obtained for the three electrode materials, the NiOOH  
286 electrode showed the maximum current density in the electro-oxidation of P1000 lignin.





289

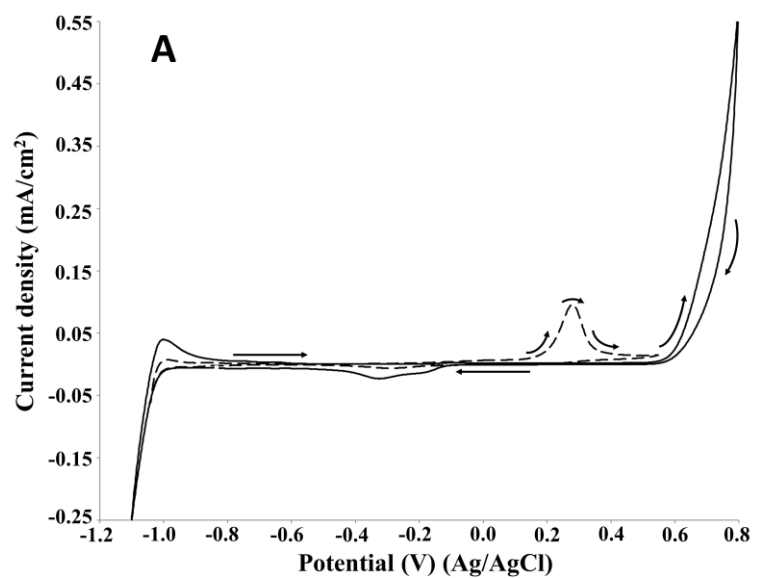
290 **Fig. 4** Cyclic voltammetry of 2 g/L P1000 lignin in 1 M NaOH (pH 14).  
 291 Voltammograms recorded at 10 mV/s on platinum (A), NiOOH (B), and graphite (C)  
 292 electrodes at room temperature. Solid line: control; dashed line: lignin.

293

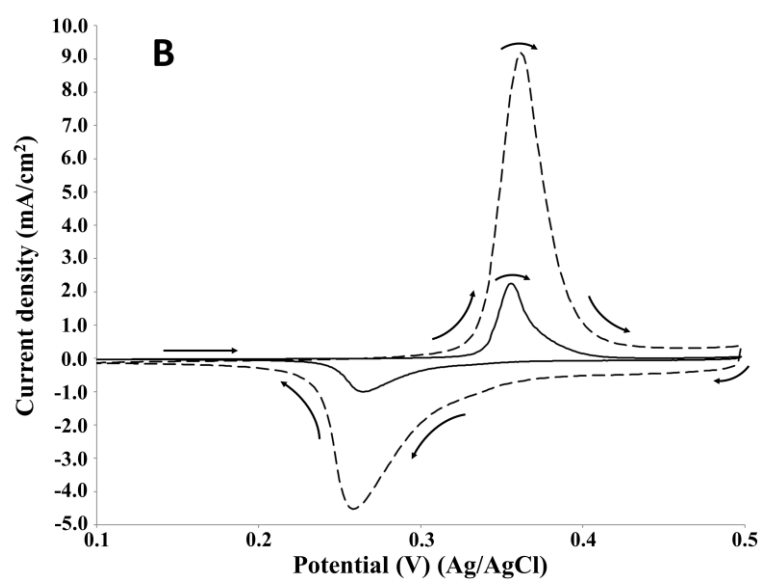
294 In order to confirm the attribution of the increase in the current density of the oxidation  
 295 peak to the lignin oxidation on the NiOOH, the same cyclic voltammetry study was  
 296 performed on guaiacol, which is one of the main structural units of lignin. **Guaiacol,**  
 297 **being a monomer, is not involved in the oxidative depolymerisation process of lignin**  
 298 **but its use can provide useful information on the performances of several electrode**  
 299 **materials in terms of electrode stability, current density and reproducibility of the**  
 300 **electrochemical reaction. Moreover, guaiacol represents a common model compound**  
 301 **used for the study of the oxidation of phenolic groups which are typical of the lignin**  
 302 **structure.**<sup>32</sup> Electrochemical oxidation of guaiacol on Pt, Au, Ti/Sb-SnO<sub>2</sub>, Ti/Pb<sub>3</sub>O<sub>4</sub>, Ni,  
 303 vitreous carbon and oxides of cobalt electrodes has been investigated in previous  
 304 studies.<sup>32, 35, 36</sup> According to the literature, the cyclic voltammetry of guaiacol is  
 305 characterised by a first irreversible discharge involving one or two electrons leading to



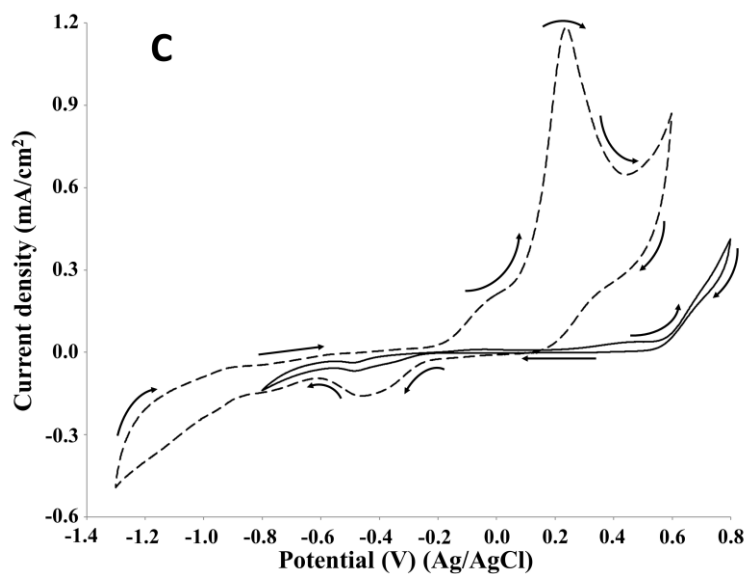
306 the formation of a radical species. In particular, in the presence of an acidic medium, the  
307 electrochemical mechanism involves two electrons, while in an alkaline medium a one-  
308 electron discharge is favoured.<sup>32, 35</sup> Fig. 5 shows the voltammograms acquired for each  
309 electrode of the present investigation.



310



311



312

313 **Fig. 5** Cyclic voltammetry of 2 g/L guaiacol in 1 M NaOH (pH 14). Voltammograms  
 314 recorded at 10 mV/s on platinum (A), NiOOH (B), and graphite (C) electrodes at room  
 315 temperature. Solid line: control; dashed line: guaiacol.

316

317 Differently from lignin, on Pt electrode only one oxidation peak was observed at around  
 318 0.3 V, which corresponded to the first peak registered for lignin. The obtained  
 319 voltammogram agreed with the information reported in the literature for the Pt electrode  
 320 in alkaline medium.<sup>37</sup> The net current density was around 0.1 mA/cm<sup>2</sup>, namely  
 321 significantly higher respect to the values obtained for the lignin oxidation. On the  
 322 NiOOH electrode, the presence of one oxidation peak at around 0.4 V was confirmed.  
 323 Similarly to the lignin oxidation, the current density of the oxidation peak of guaiacol  
 324 was significantly higher than the control test. For the guaiacol electro-oxidation, the net  
 325 current density was 7 mA/cm<sup>2</sup>, namely 3.5-folds higher than the value registered for the  
 326 lignin oxidation (2 mA/cm<sup>2</sup>). Moreover, the net charge density of the oxidation and  
 327 reduction peaks were 0.8 and 0.4 mC/cm<sup>2</sup>, respectively. Also on the graphite electrode,  
 328 one oxidation peak was observed at around 0.3 V, according to the behaviour of Pt and

329 NiOOH electrocatalysts. Moreover, the potential agreed with the value acquired for the  
330 lignin oxidation. The net current density of the peak was around  $1.2 \text{ mA/cm}^2$ , namely 3-  
331 folds higher than the value registered for the lignin oxidation ( $0.5 \text{ mA/cm}^2$ ). The cyclic  
332 voltammetry study on the guaiacol electro-oxidation confirmed the NiOOH as the best  
333 electrodes among those tested in terms of current density.

334

### 335 **3.2 Cyclic voltammetry study - effect of scan rate**

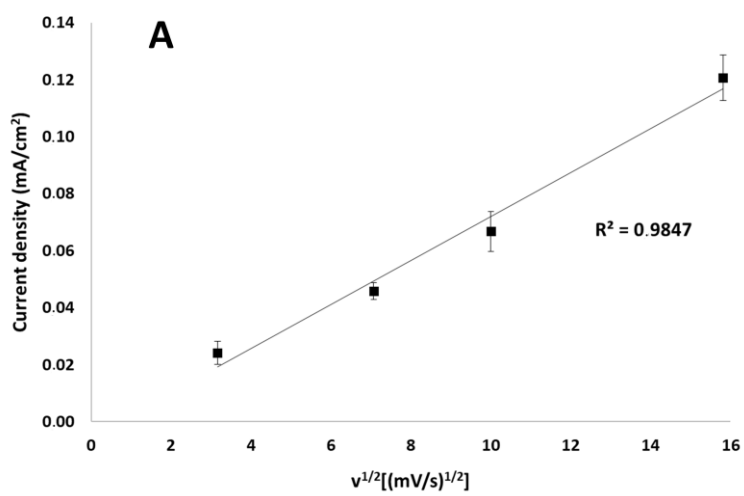
336 In order to establish if the electro-oxidation of P1000 lignin is mass transfer controlled,  
337 the effect of the scan rate of the three electrodes at pH 14 in the presence of 2 g/L lignin  
338 was investigated. For all the electrodes a linear relation was obtained by relating the  
339 current density of the lignin oxidation peak with the squared root of the scan rate (Fig.  
340 6). This linear relationship is an indication that the investigated process is mass transfer  
341 controlled, according to the Randles-Sevcik equation:<sup>38</sup>

$$342 I_p = 0.4463 \cdot z \cdot F \cdot A \cdot C \cdot [(z \cdot F \cdot v \cdot D)/(R \cdot T)]^{1/2}$$

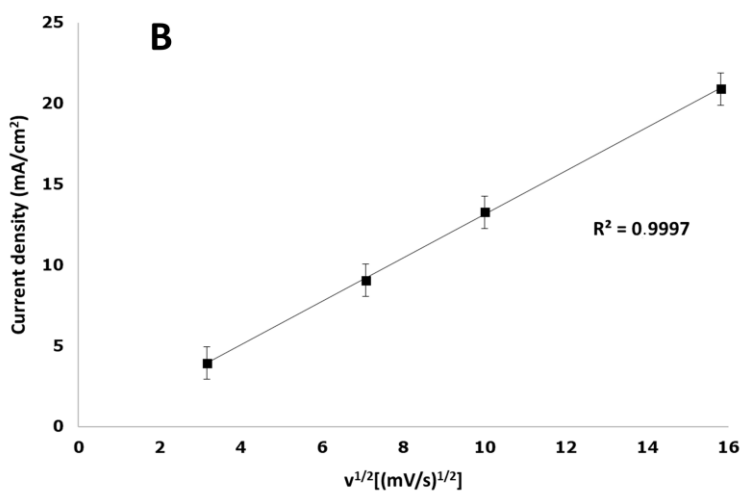
343 that at 25 °C can be expressed according to the following equation:

$$344 I_p = 2.686 \cdot 10^5 \cdot z^{3/2} \cdot A \cdot D^{1/2} \cdot C \cdot v^{1/2}$$

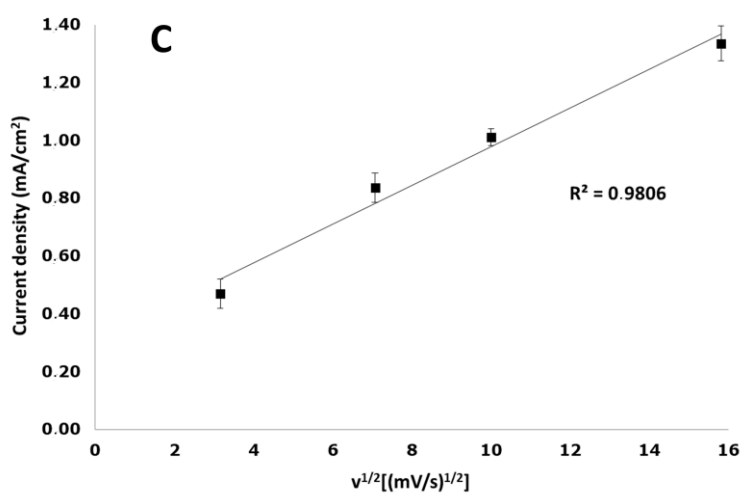
345 where  $I_p$  is the current density (A),  $z$  is the number of electrons exchanged,  $F$  is the  
346 Faraday constant (96485 C/mol),  $A$  is the area of the electrode ( $\text{cm}^2$ ),  $C$  is the initial  
347 concentration of the analyte ( $\text{mol/cm}^3$ ),  $v$  is the potential scan rate (V/s),  $D$  is the  
348 diffusion coefficient of the analyte ( $\text{cm}^2/\text{s}$ ),  $R$  is the gas constant (J/mol·K) and  $T$  is the  
349 temperature (K).



350



351



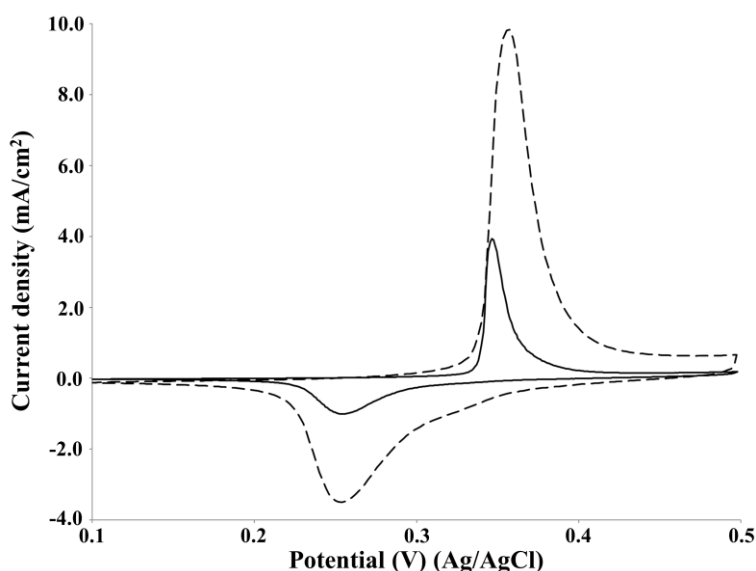
352

353 **Fig. 6** Current density ( $\text{mA}/\text{cm}^2$ ) as a function of the square root of scan rate in cyclic  
354 voltammetry measurements of 2 g/L P1000 lignin at pH 14 on platinum (A), NiOOH  
355 (B), and graphite (C) electrodes at room temperature.

356

### 357 3.3 Cyclic voltammetry study - effect of lignin concentration

358 The effect of the increase in the lignin concentration on the current density of the  
359 oxidation peak was investigated by cyclic voltammetry on the NiOOH electrode at pH  
360 14 (Fig. 7).



361

362 **Fig. 7** Cyclic voltammetry of P1000 lignin at the concentration of 2 g/L (solid line) and  
363 20 g/L (dashed line). Voltammograms recorded at 10 mV/s on NiOOH electrode at  
364 room temperature.

365

366 The increase of lignin concentration from 2 to 20 g/L resulted in a 2.5-folds increase of  
367 the current density of the oxidation peak of P1000 lignin from 4 to around  $10 \text{ mA}/\text{cm}^2$ .

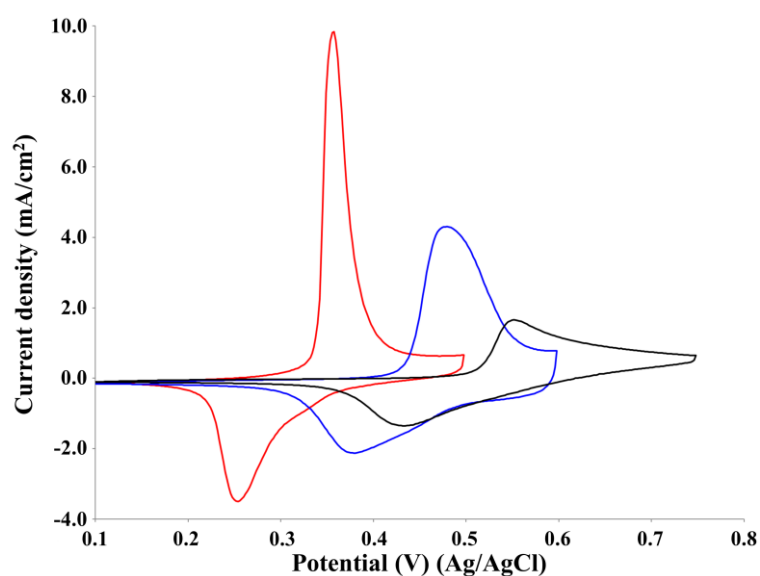
368 A similar increase of the electrode activity with increasing of lignin concentration was  
369 obtained by Cai et al. in the cyclic voltammetry, adopting different concentrations in the

370 range 20-40 g/L on Pb/PbO<sub>2</sub> electrode in alkali solution.<sup>23</sup> Moreover, the same  
371 phenomenon is reported in the literature for the electrochemical oxidation of guaiacol<sup>35</sup>  
372 and urea on the NiOOH electrode in alkaline media.<sup>39</sup>

373

### 374 3.4 Cyclic voltammetry study - effect of pH

375 The effect of pH on the oxidative potential of P1000 lignin was investigated by  
376 cyclic voltammetry on the NiOOH electrocatalyst (Fig. 8).



377

378 **Fig. 8** Cyclic voltammetry of 2 g/L P1000 lignin at pH 12 (black line), 13 (blue line)  
379 and 14 (red line). Voltammograms recorded at 50 mV/s on NiOOH electrode at room  
380 temperature.

381

382 The pH increase resulted in a decrease in the potential of the lignin oxidation peak  
383 according to the Nernst equation.<sup>40, 41</sup> It was around 0.55 V at pH 12, around 0.45 V at  
384 pH 13 and around 0.35 V at pH 14. Similar results were obtained by Vedharathinam and  
385 Botte for the electrochemical oxidation of urea on NiOOH electrode in alkaline media.<sup>39</sup>  
386 Moreover, the increase in pH resulted in an increase of the peak current density which is

387 related to the kinetics of the oxidation current for Ni(OH)<sub>2</sub>/NiOOH according to the  
388 literature.<sup>42, 43</sup> In particular, since the lignin oxidation is catalysed by NiOOH species  
389 and the formation of this last one on the electrode surface is strongly affected by the  
390 OH<sup>-</sup> activity, the increase of pH, namely the increase of OH<sup>-</sup> concentration, increases  
391 the anodic current density.<sup>39</sup> In fact, it was around 1 mA/cm<sup>2</sup> at pH 12, around 4  
392 mA/cm<sup>2</sup> at pH 13 and around 10 mA/cm<sup>2</sup> at pH 14. The net charge density of the  
393 oxidation peaks at pH 12, 13 and 14 were 3.1, 5.3 and 5.3 mC/cm<sup>2</sup>, respectively. The  
394 net charge density of the reduction peaks at pH 12, 13 and 14 were 2.8, 3.8 and 3.6  
395 mC/cm<sup>2</sup>, respectively. The increase of pH from 12 to 13 or 14 determined an increase of  
396 71% of the charge density of the oxidation peak, corresponding to 2.2 mC/cm<sup>2</sup>. The  
397 same effect of the pH increase on the current density was observed by Cai et al. in the  
398 cyclic voltammetry of Pb/PbO<sub>2</sub> in alkali solution for the commercial corn stover  
399 lignin.<sup>23</sup> Based on the results obtained, pH 14 was selected as the optimal reaction  
400 condition for P1000 lignin electrolysis. This reaction condition agreed with the  
401 information reported in the literature for the electro-oxidative depolymerisation of other  
402 technical lignins.<sup>13, 23, 32</sup>

403 Considering the performances of Pt, NiOOH and graphite electrodes and the results  
404 obtained by the preliminary cyclic voltammetry study, the following reaction conditions  
405 were selected for the electrolysis of P1000 lignin: NiOOH electrode, pH 14, 0.4 V, 20  
406 g/L lignin. NiOOH was selected as the most efficient electrocatalyst based on the  
407 highest net current density registered for the lignin oxidation peak in the cyclic  
408 voltammetry.

409

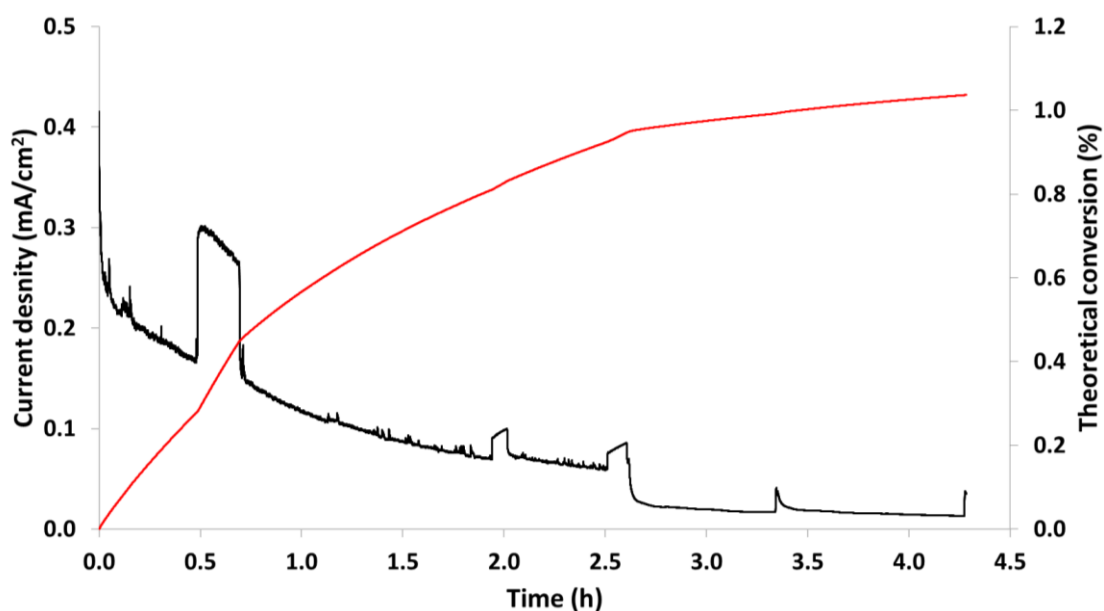
### 410 **3.5 Electrolysis of lignin**

411 The initial cyclic voltammetry study aimed at a preliminary screening for  
412 determining the optimal reaction conditions for the electrolysis of soda P1000 lignin in  
413 order to produce added-value aromatic compounds. NiOOH electrode showed the  
414 maximum current density in the electro-oxidation of P1000 lignin during the cyclic  
415 voltammetry study. In particular, by comparing the current density at the maximum  
416 oxidative potential value for each electrode, on NiOOH electrode the current density  
417 increased to around  $2 \text{ mA/cm}^2$  at 0.35 V, while on graphite and platinum electrodes it  
418 increased to around  $0.5 \text{ mA/cm}^2$  and  $23 \text{ }\mu\text{A/cm}^2$  at 0.2 V, respectively. Besides, for all  
419 the three materials, the electro-oxidation of P1000 lignin resulted mass transfer  
420 controlled. Finally, nickel, as well as graphite, represents a cheaper material than  
421 platinum and it is characterised by better mechanical properties than graphite, especially  
422 in terms of brittleness. Based on all these results and considerations, NiOOH was  
423 selected as the preferred electrode material for the following constant-potential lignin  
424 electrolysis in water. Alkaline solutions are typically used to dissolve lignin favouring  
425 its oxidative depolymerisation.<sup>34, 44</sup> In the literature, several hypotheses on the oxidation  
426 mechanism of lignin to give valuable aromatics are reported.<sup>22, 32, 45</sup> In the case of  
427 electro-oxidative depolymerisation, the R–O–R ether linkages, which are thermally and  
428 oxidatively more labile with respect to the C–C linkages, are firstly involved in the  
429 mechanism.<sup>46</sup> Mechanistic studies found the C–O bond of the abundant  $\beta$ –O–4 aryl  
430 ether linkage is cleaved by the electrocatalyst.<sup>22</sup> Subsequently, the same electrode  
431 material is able to cleave  $C_\alpha$ – $C_\beta$  bonds in the electro-oxidation of  $\beta$ –O–4 linkages.<sup>21</sup>  
432 Moreover, the cleavage of  $C_\alpha$ – $C_\beta$  bonds competes with the  $C_\alpha$ –carbonylation reaction.<sup>19</sup>  
433 The ether bonds breaking leads to the formation of oxygenated aromatics such as  
434 vanillin, vanillic acid, vanillin acetate and guaiacol. Moreover, during electrolysis in



435 alkaline solution, different substituted phenolates are produced, which are involved in a  
436 direct electron transfer leading to the synthesis of radical species which take part in the  
437 lignin depolymerisation.<sup>32</sup> Recently, Chen et al. studied the electrochemical oxidation  
438 mechanisms for the C–O and C–C cleavages of  $\beta$ -O-4 linkages in lignin model  
439 monomers and dimers such as 2-phenoxy-1-phenethanol, 2-phenoxyacetophenone and  
440 2-phenoxy-1-phenylethane.<sup>47</sup> Authors demonstrated that the conversions of aryl ring in  
441 the lignin model dimers are involved in the starting single electron transfer oxidations,  
442 forming their benzene radical cation intermediates. Then, these last ones process further  
443 chemical conversion on their  $\beta$ -O-4 bonds due to electron delocalisation, resulting in  
444 cationic products and the phenolic radical. The cationic products are finally transformed  
445 into alcohol products.<sup>47</sup>

446 Fig. 9 shows the results of the P1000 lignin electro-oxidative depolymerisation under  
447 the optimal reaction conditions.



448  
449 **Fig. 9** Constant potential electrolysis of 20 g/L P1000 lignin on NiOOH electrode at pH  
450 14, 0.4 V and room temperature. Black line: current density (mA/cm<sup>2</sup>); Red line:  
451 theoretical conversion (%).

452

453 In particular, Fig. 9 shows the variation of the current density (mA/cm<sup>2</sup>), black line, and  
454 the theoretical conversion (%), red line, as a function of the reaction time. At the end of  
455 the reaction, the theoretical conversion was 1.0%, which represented the oxidation  
456 degree of the implemented process. The severe current density decreasing observed in  
457 Fig. 9 was related to the passivation of the electrode. This phenomenon is due to the  
458 lignin adsorbed on the electrode occupying the active site of hydroxyl radicals, which  
459 changed the electrochemical resistance. Moreover, in Fig. 9 the flat-topped peaks in the  
460 black line represent artefacts related to the sampling at different reaction time. In fact,  
461 the sample taking generated a temporary de-passivation of the electrode increasing the  
462 current density for a short time before the following passivation of the surface. Future  
463 outlooks of the present preliminary investigation will be focused on the resolution of the  
464 electrode passivation, by testing a different electrochemical cell polarity and/or a higher  
465 electrode area.

466 Table 1 reports the list of the identified aromatic compounds and their concentrations  
467 obtained after the P1000 electrolysis.

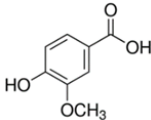
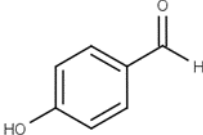
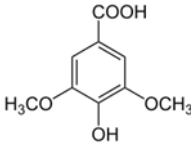
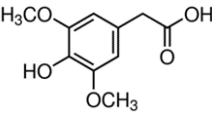
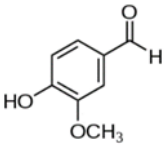
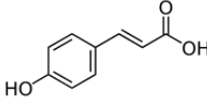
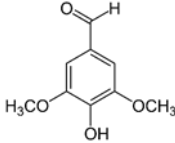
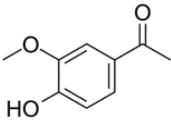
468

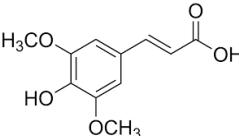
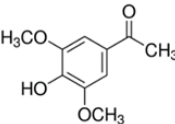
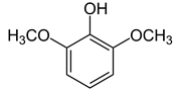
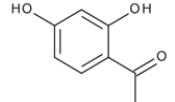
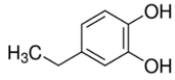
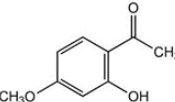
469 **Table 1** List of aromatic compounds produced after the electro-oxidative  
470 depolymerisation of soda P1000 lignin on NiOOH electrode under the optimal reaction  
471 conditions among those investigated (20 g/L P1000 lignin, NiOOH electrode, pH 14,  
472 0.4 V, room temperature).

---

| Number | Compound | Structure | Concentration<br>(mg/L) | Yield <sup>a</sup><br>(wt%) |
|--------|----------|-----------|-------------------------|-----------------------------|
|--------|----------|-----------|-------------------------|-----------------------------|

---

|   |  |   |      |      |
|---|--|---|------|------|
| 1 | Vanillic acid                            |    | 23.4 | 0.12 |
| 2 | 4-hydroxybenzaldehyde                    |    | 17.3 | 0.09 |
| 3 | Syringic acid                            |    | 20.6 | 0.10 |
| 4 | 3,5-dimethoxy-4-hydroxyphenylacetic acid |   | 2.8  | 0.01 |
| 5 | Vanillin                                 |  | 23.8 | 0.12 |
| 6 | <i>p</i> -Coumaric acid                  |  | 18.2 | 0.09 |
| 7 | 3,5-dimethoxy-4-hydroxybenzaldehyde      |  | 13.3 | 0.07 |
| 8 | Acetovanillone                           |  | 30.2 | 0.15 |

|    |                                     |   |      |      |
|----|-------------------------------------|---|------|------|
| 9  | Sinapic acid                        |    | 64.3 | 0.32 |
| 10 | 3,5-dimethoxy-4-hydroxyacetophenone |    | 9.9  | 0.05 |
| 11 | 2,6-dimethoxyphenol                 |    | 14.1 | 0.07 |
| 12 | 2,4-dihydroxyacetophenone           |    | 0.1  | 0.00 |
| 13 | 4-ethylcatechol                     |   | 5.1  | 0.03 |
| 14 | 2-hydroxy-4-methoxyacetophenone     |  | 2.6  | 0.01 |

473 <sup>a</sup> Products yield was calculated with respect to the lignin loading in the electrochemical  
474 cell.

475

476 14 added-value bioproducts were identified (Table 1). The main products were sinapic  
477 acid (64.3 mg/L, 0.32 wt%), acetovanillone (30.2 mg/L, 0.15 wt%), vanillin (23.8 mg/L,  
478 0.12 wt%) and vanillic acid (23.4 mg/L, 0.12 wt%). The sum of aromatics  
479 concentrations resulted 245.7 mg/L, corresponding to a production of around 1.2 kg of  
480 aromatics from 100 kg of P1000 lignin. This yield value of 1.23 wt% is in line with the  
481 literature. In fact, according to Weber and Ramasamy, mass yields are typically  $\leq 2$   
482 wt%.<sup>46</sup> For example, Di Marino et al. obtained 14 aromatic compounds with an overall

483 yield of 2.0 wt% respect to the starting lignin,<sup>25</sup> while Ghahremani and Staser identified  
484 4 products with an overall yield of 0.2 wt% respect to the starting lignin.<sup>48</sup> Moreover,  
485 similar aromatic bioproducts were obtained in the study of Long et al.<sup>49</sup> on the chemical  
486 depolymerisation of organosolv pine lignin and in the study of Yang et al.<sup>50</sup> on the  
487 enzymatic depolymerisation of Kraft lignin. The amount of products corresponds with  
488 the estimated maximum conversion and therefore indicates a high coulombic efficiency  
489 for the depolymerisation of P1000 lignin.

490

#### 491 **4. Conclusions**

492 In the present study, for the first time, the electro-oxidative depolymerisation of soda  
493 P1000 lignin into added-value aromatic compounds was **preliminarily** investigated. In  
494 particular, three anode materials were tested, Pt, NiOOH and graphite, as well as three  
495 pH values, 12, 13 and 14 and two lignin concentrations, 2 and 20 g/L. The preliminary  
496 cyclic voltammetry study allowed us to identify the optimal reactions conditions for the  
497 lignin electrolysis. NiOOH, pH 14, 20 g/L lignin and 0.4 V resulted the best reaction  
498 conditions **among those tested**. Adopting these parameters, the constant potential  
499 electrolysis of P1000 lignin was performed into a divided cell in the presence of an  
500 anion exchange membrane. 14 main aromatic compounds were identified and quantified  
501 by UPLC-MS. The main products were sinapic acid, acetovanillone, vanillin and  
502 vanillic acid, achieving the overall oxidation degree of 1%. The future investigations  
503 will aim to **avoid the electrode passivation and to** increase the oxidation of soda P1000  
504 lignin in order to raise the aromatics yield.

505

#### 506 **Author contributions**

507 **Nicola Di Fidio:** Methodology, Investigation, Data curation, Formal analysis,  
508 Writing - original draft. **Johan W. Timmermans:** Methodology, Formal analysis,  
509 Supervision. **Claudia Antonetti:** Writing - review & editing, Formal analysis. **Anna**  
510 **Maria Raspolti Galletti:** Writing - review & editing, Formal analysis, Supervision.  
511 **Richard J. A. Gosselink:** Conceptualization, Writing - review & editing, Supervision,  
512 Funding acquisition, Resources. **Roel J. M. Bisselink:** Conceptualization,  
513 Methodology, Formal analysis, Writing - review & editing, Supervision. **Ted M.**  
514 **Slaghek:** Conceptualization, Writing - review & editing, Supervision, Funding  
515 acquisition, Resources.

516

## 517 **Conflict of interest**

518 There are no conflicts to declare.

519

## 520 **Acknowledgements**

521 The contribution of COST Action LignoCOST (CA17128), supported by COST  
522 (European Cooperation in Science and Technology), in promoting interaction, exchange  
523 of knowledge and collaborations in the field of lignin valorisation, is gratefully  
524 acknowledged. The contribution of COST Action LignoCOST in supporting the present  
525 work by a Short-Term Scientific Mission (Call No. 1, 2<sup>nd</sup> Grant Period) is  
526 acknowledged. Federico Maria Vivaldi of the Department of Chemistry and Industrial  
527 Chemistry of the University of Pisa is gratefully acknowledged for the fruitful  
528 discussion and his suggestions about the data elaboration.

529

## 530 **References**

- 531 1. I. De Bari, D. Cuna and N. Di Fidio, in *Biofuels Production and Processing*  
532 *Technology*, eds. M. Riazi and D. Chiaramonti, CRC Press, Boca Raton, 2017,  
533 DOI: 10.1201/9781315155067, ch. 19, pp. 533-561.
- 534 2. N. Di Fidio, S. Fulignati, I. De Bari, C. Antonetti and A. M. Raspolli Galletti,  
535 *Bioresource Technology*, 2020, **313**, 123650-123658.
- 536 3. V. K. Garlapati, A. K. Chandel, S. J. Kumar, S. Sharma, S. Sevda, A. P. Ingle  
537 and D. Pant, *Renewable and Sustainable Energy Reviews*, 2020, **130**, 109977-  
538 109989.
- 539 4. S. Constant, H. L. Wienk, A. E. Frissen, P. de Peinder, R. Boelens, D. S. Van  
540 Es, R. J. Grisel, B. M. Weckhuysen, W. J. Huijgen and R. J. A. Gosselink,  
541 *Green Chemistry*, 2016, **18**, 2651-2665.
- 542 5. C. Li, X. Zhao, A. Wang, G. W. Huber and T. Zhang, *Chemical reviews*, 2015,  
543 **115**, 11559-11624.
- 544 6. Z. Zhang, J. Song and B. Han, *Chemical reviews*, 2017, **117**, 6834-6880.
- 545 7. T. Li, H. Ma, S. Wu and Y. Yin, *Energy Conversion and Management*, 2020,  
546 **207**, 112551-112560.
- 547 8. J. Dillies, C. Vivien, M. Chevalier, A. Rulence, G. Châtaigné, C. Flahaut, V.  
548 Senez and R. Froidevaux, *Biotechnology and Applied Biochemistry*, 2020, **67**,  
549 774-782.
- 550 9. P. J. De Wild, W. J. Huijgen and R. J. A. Gosselink, *Biofuels, Bioproducts and*  
551 *Biorefining*, 2014, **8**, 645-657.
- 552 10. Z. Sun, B. Fridrich, A. de Santi, S. Elangovan and K. Barta, *Chemical reviews*,  
553 2018, **118**, 614-678.

- 554 11. F. Bateni, R. Ghahremani and J. A. Staser, *Journal of Applied Electrochemistry*,  
555 2021, **51**, 65-78.
- 556 12. X. Du, H. Zhang, K. P. Sullivan, P. Gogoi and Y. Deng, *ChemSusChem*, 2020,  
557 **13**, 4318-4343.
- 558 13. S. Singh and H. R. Ghatak, *Journal of Wood Chemistry and Technology*, 2017,  
559 **37**, 407-422.
- 560 14. D. Di Marino, V. Aniko, A. Stocco, S. Kriescher and M. Wessling, *Green*  
561 *Chemistry*, 2017, **19**, 4778-4784.
- 562 15. S. Singh and H. R. Ghatak, *Holzforschung*, 2018, **72**, 187-199.
- 563 16. B. Joffres, C. Lorentz, M. Vidalie, D. Laurenti, A. A. Quoineaud, N. Charon, A.  
564 Daudin, A. Quignard and C. Geantet, *Applied Catalysis B: Environmental*, 2014,  
565 **145**, 167-176.
- 566 17. X. Huang, T. I. Korányi, M. D. Boot and E. J. Hensen, *ChemSusChem*, 2014, **7**,  
567 2276-2288.
- 568 18. J. Pu, D. Laurenti, C. Geantet, M. Tayakout-Fayolle and I. Pitault, *Chemical*  
569 *Engineering Journal*, 2020, **386**, 122067-122067.
- 570 19. T. Shiraishi, T. Takano, H. Kamitakahara and F. Nakatsubo, *Holzforschung*,  
571 2012, **66**, 303-309.
- 572 20. J. Gierer and I. Norén, *Holzforschung-International Journal of the Biology,*  
573 *Chemistry, Physics and Technology of Wood*, 1980, **34**, 197-200.
- 574 21. E. Baciocchi, M. Bietti and O. Lanzalunga, *Accounts of chemical research*,  
575 2000, **33**, 243-251.
- 576 22. V. L. Pardini, C. Z. Smith, J. H. Utley, R. R. Vargas and H. Viertler, *The*  
577 *Journal of Organic Chemistry*, 1991, **56**, 7305-7313.



- 578 23. P. Cai, H. Fan, S. Cao, J. Qi, S. Zhang and G. Li, *Electrochimica Acta*, 2018,  
579 **264**, 128-139.
- 580 24. Y. Jia, Y. Wen, X. Han, J. Qi, Z. Liu, S. Zhang and G. Li, *Catalysis Science &*  
581 *Technology*, 2018, **8**, 4665-4677.
- 582 25. D. Di Marino, D. Stöckmann, S. Kriescher, S. Stiefel and M. Wessling, *Green*  
583 *Chemistry*, 2016, **18**, 6021-6028.
- 584 26. H. Zhu, Y. Chen, T. Qin, L. Wang, Y. Tang, Y. Sun and P. Wan, *Rsc Advances*,  
585 2014, **4**, 6232-6238.
- 586 27. M. Shestakova and M. Sillanpää, *Reviews in Environmental Science and*  
587 *Bio/Technology*, 2017, **16**, 223-238.
- 588 28. R. Latsuzbaia, R. Bisselink, A. Anastasopol, H. Van der Meer, R. Van Heck, M.  
589 Segurola Yagüe, M. Zijlstra, M. Roelands, M. Crockatt and E. Goetheer,  
590 *Journal of Applied Electrochemistry*, 2018, **48**, 611-626.
- 591 29. T. K. Dier, D. Rauber, D. Durneata, R. Hempelmann and D. A. Volmer,  
592 *Scientific reports*, 2017, **7**, 1-12.
- 593 30. S. Stiefel, A. Schmitz, J. Peters, D. Di Marino and M. Wessling, *Green*  
594 *Chemistry*, 2016, **18**, 4999-5007.
- 595 31. G. Milczarek, *Electroanalysis: An International Journal Devoted to*  
596 *Fundamental and Practical Aspects of Electroanalysis*, 2007, **19**, 1411-1414.
- 597 32. P. Parpot, A. Bettencourt, A. Carvalho and E. Belgsir, *Journal of applied*  
598 *electrochemistry*, 2000, **30**, 727-731.
- 599 33. O. Movil-Cabrera, A. Rodriguez-Silva, C. Arroyo-Torres and J. A. Staser,  
600 *Biomass and Bioenergy*, 2016, **88**, 89-96.

- 601 34. A. Caravaca, W. E. Garcia-Lorefice, S. Gil, A. de Lucas-Consuegra and P.  
602 Vernoux, *Electrochemistry Communications*, 2019, **100**, 43-47.
- 603 35. Y. Samet, R. Abdelhedi and A. Savall, *Phys. Chem. News*, 2002, **8**, 89-99.
- 604 36. D. Shao, W. Chu, X. Li, W. Yan and H. Xu, *RSC advances*, 2016, **6**, 4858-4866.
- 605 37. S. J. Reddy and V. Krishnan, *Indian Journal of Chemistry*, 1978, **16**, 684-687.
- 606 38. J. J. Van Benschoten, J. Y. Lewis, W. R. Heineman, D. A. Roston and P. T.  
607 Kissinger, *Journal of Chemical Education*, 1983, **60**, 772.
- 608 39. V. Vedharathinam and G. G. Botte, *Electrochimica Acta*, 2012, **81**, 292-300.
- 609 40. M. M. Walczak, D. A. Dryer, D. D. Jacobson, M. G. Foss and N. T. Flynn,  
610 *Journal of chemical education*, 1997, **74**, 1195.
- 611 41. F. Vivaldi, D. Santalucia, N. Poma, A. Bonini, P. Salvo, L. Del Noce, B. Melai,  
612 A. Kirchhain, V. Kolivoška, R. Sokolova, M. Hromadová and F. Di Francesco,  
613 *Sensors and Actuators B: Chemical*, 2020, **322**, 128650-128658.
- 614 42. P. Robertson, *Journal of Electroanalytical Chemistry and Interfacial*  
615 *Electrochemistry*, 1980, **111**, 97-104.
- 616 43. J. Kaulen and H. J. Schäfer, *Tetrahedron*, 1982, **38**, 3299-3308.
- 617 44. M. Zirbes, D. Schmitt, N. Beiser, D. Pitton, T. Hoffmann and S. R. Waldvogel,  
618 *ChemElectroChem*, 2019, **6**, 155-161.
- 619 45. V. Tarabanko, D. Petukhov and G. Selyutin, *Kinetics and catalysis*, 2004, **45**,  
620 569-577.
- 621 46. R. S. Weber and K. K. Ramasamy, *ACS omega*, 2020, **5**, 27735-27740.
- 622 47. J. Chen, H. Yang, H. Fu, H. He, Q. Zeng and X. Li, *Physical Chemistry*  
623 *Chemical Physics*, 2020, **22**, 11508-11518.
- 624 48. R. Ghahremani and J. A. Staser, *Holzforschung*, 2018, **72**, 951-960.

- 625 49. J. Long, Y. Xu, T. Wang, Z. Yuan, R. Shu, Q. Zhang and L. Ma, *Applied*  
626 *Energy*, 2015, **141**, 70-79.
- 627 50. Y. Yang, W. Y. Song, H. G. Hur, T. Y. Kim and S. Ghatge, *International*  
628 *journal of biological macromolecules*, 2019, **124**, 200-208.